科学通报 2017 年 第 62 卷 第 12 期：1278 ~ 1284
论 文
《中国科学》杂志社
SCIENCE CHINA PRESS

类血红细胞状氧化铁纳米颗粒在小鼠大脑皮层光声成像中的应用

何再乾[1]，王一平[1]，闫晓乐[1]，杨敏敏[1]，王颖[2]，李朋伟[1*]，蒋华北[3]，张文栋[1]

1. 太原理工大学信息工程学院微纳系统研究中心，新型传感器和智能控制系统教育部重点实验室，太原 030024;
2. 太原理工大学力学学院生物医学系，太原 030024;
3. Department of Medical Engineering, University of South Florida, Tampa, 32611, USA
* 联系人, E-mail: lipengwei@tyut.edu.cn

2016-12-27 收稿, 2017-02-09 修回, 2017-02-24 接受, 2017-03-30 网络版发表
国家自然科学基金(11602159)、山西省优秀人才科技创新项目(201605D211020)和山西省高等学校科技创新项目(2016136)资助

摘要 制备了盐酸多巴胺修饰的类血红细胞状氧化铁纳米颗粒(DA@Fe_2O_3)，基于其良好的光吸收特性，讨论了其作为光声造影剂的可能性．对DA@Fe_2O_3进行了体外细胞毒性测试，不同浓度材料光声信号响应和体外光声造影增强特性测试等；在此基础上，研究了其对小鼠大脑皮层血管的光声造影效果．结果表明，DA@Fe_2O_3生物兼容性良好、体外光声性能和造影效果优异，在小鼠大脑皮层血管中能起到较好的光声造影增强作用，具有成为高性能光声造影剂的潜质．

关键词 氧化铁纳米颗粒，造影剂，光声成像

光声成像(PAT)是近年来兴起的一种典型的生物医学成像技术，其结合了纯光学成像的高对比度和超声成像探测深度好的优点，与正电子断层扫描(PET)、X射线扫描，核磁共振扫描(MRI)等[1]传统生物成像技术相比，具有非侵入、非电离、高穿透和低成本的特性，能够获得较高质量的分子影像效果．光声成像技术源于光声效应，即当周期性电磁波照射生物组织时，组织中的内源性吸收体(如血红蛋白、黑色素)吸收光能产生热弹效应，并向外释放超声波，然后利用组织周围的探测装置(超声换能器)接收超声信号，并将其转化成电信号最终重建获得图像[2]．利用光声传感技术可以体外对活体进行血氧浓度监测、脑组织成像、肿瘤血管监测等[3~6]．然而，由于激光较强的散射效应，光声信号的信噪比会随其穿透深度的增加而大幅衰减．光声造影剂作为一种改变局域组织光吸收特性的成像助剂，可以从本源上增强光声信号，提高光声成像的对比度和分辨率．相关研究也逐步成为光声成像、光热治疗等领域的热点之一．

近年来，纳米材料以其独特的光学性质、易控的表面化学能力，被广泛用作外源性光声造影剂[7~9]．目前常见的光声造影剂有金纳米材料、碳纳米材料、过渡金属硫化物等无机纳米材料．例如，Kim等人[10]研究了聚乙二醇(PEG)修饰的金纳米笼作为造影剂来增强小鼠体内黑色素瘤的成像效果．Kang等人[11]利用壳聚糖修饰的纳米碳管对癌细胞进行光热治疗．苏州大学刘庄课题组[12~14]探讨了石墨烯材料、过渡金属硫化物(MoS_2)作为近红外光声探针进行小鼠肿瘤有效光热治疗的可行性．然而，尽管无机纳米材料具有良好的光声效应，但其生物兼容性问题还有待

引用格式: 何再乾，王一平，闫晓乐，等．类血红细胞状氧化铁纳米颗粒在小鼠大脑皮层光声成像中的应用．科学通报, 2017, 62: 1278–1284
He Z Q, Wang Y P, Yan X L, et al. Red blood cell-like-Fe_2O_3 nanocrystals as contrast agents for PAT on a rat cerebral cortex *in vivo* (in Chinese). Chin Sci Bull, 2017, 62: 1278–1284, doi: 10.1360/N972016-01455

© 2017《中国科学》杂志社

进一步研究和解决. 无毒化、低成本的光声造影剂研究是目前该领域的研究热点. 氧化铁, 作为一种典型的过渡金属氧化物, 具有良好的磁性、热稳定性和化学稳定性, 成本低, 尤其具有生物组织低毒(血红蛋白中富含铁离子)、兼容性好等特性, 被广泛用作MRI等生物医学成像造影剂[15,16], 同时也是光声成像、光热治疗助剂的潜在应用材料[17,18]. 另外, 为了提高无机纳米材料的生物兼容性, 并且使其更容易与特定抗体结合, 具有肿瘤定位、药物输运等功能, 对其进行生物功能化也是必不可少的. 常见的可用于对无机纳米材料进行生物功能化的有机活性材料有PEG、叶酸(FA)、多巴胺(DA)等. 盐酸多巴胺含有邻二苯酚基团、氨基、羟基, 其中邻二苯酚基团极易被氧化产生半醌自由基, 然后耦合形成交联键[19~22]. 这使得多巴胺可以和有机-无机表面建立共价和非共价的相互作用, 其表面更容易与大多数生物分子结合, 为其作为定向光声造影剂、光热治疗剂等提供了可能.

本文合成了盐酸多巴胺修饰的类血红细胞状氧化铁纳米颗粒(DA@Fe_2O_3), 选取小鼠胚胎成纤维细胞NIH3T3作为生物样本, 检测了其生物毒性和细胞增殖情况; 系统研究了合成DA@Fe_2O_3与商用金纳米颗粒作为光声造影剂的体外、体内光声信号信噪比及成像对比度等情况.

1 材料和方法

(ⅰ) 材料. 六水合氯化铁($FeCl_3·6H_2O$)、硫酸钠(Na_2SO_4)、二水合磷酸二氢钠($NaH_2PO_4·2H_2O$)、乙腈(C_2H_3N)购自国药集团化学试剂有限公司; 盐酸多巴胺(dopamine hydrochloride, $C_8H_{11}NO_2·HCl$)购自阿拉丁试剂(上海)有限公司; 金纳米颗粒(粒径约30 nm)购自星火科技纳米材料有限公司; 小鼠胚胎成纤维细胞NIH3T3购自中国医学科学院基础医学研究所基础医学细胞中心.

(ⅱ) DA@Fe_2O_3光声造影剂制备. 利用水热法合成类红细胞状Fe_2O_3纳米材料. 典型合成过程如下: 称取0.324 g(0.02 mol/L)氯化铁, 0.0047 g(0.55 mmol/L)硫酸钠以及0.05 mmol/L(称取0.048 g磷酸二氢钠配制成浓度为5 mmol/L的水溶液, 然后将其稀释100倍至浓度为0.05 mmol/L)磷酸二氢钠, 混合加入100 mL去离子水(18 MΩ)中, 搅拌至完全溶解. 将上述混合溶液放置不锈钢高温高压反应釜中, 加热至220℃, 反应5 h. 将反应产物用去离子水和酒精清洗数次后离心, 除去上层清液, 干燥直至恒重, 获得类红细胞状Fe_2O_3纳米材料.

称取0.06 g Fe_2O_3溶于2 mL乙腈溶液中, 另称取3.793 g DA溶于1 mL乙腈溶液中. 将两种溶液混合搅拌均匀后超声30 min. 反应产物用乙腈溶液和酒精清洗数次后离心, 除去上层清液, 干燥直至恒重, 获得盐酸多巴胺包覆的氧化铁纳米材料(DA@Fe_2O_3).

(ⅲ) DA@Fe_2O_3对NIH3T3细胞的毒性检测. 本实验选取正常小鼠胚胎成纤维细胞NIH3T3, 良伊格尔培养基(DMEM)高糖液体培养基孵育, 以10000/孔种于96孔板, 在37℃, 5% CO_2条件下培养. 细胞贴壁4~6 h后, 将不同浓度(3.125, 6.25, 12.5, 25, 50, 100, 200 μg/mL)各20 μL的DA@Fe_2O_3放置于96孔板, 分别孵化16和40 h. 之后用MTT比色法(噻唑蓝)检测细胞的相对存活率.

(ⅳ) 光声成像实验装置. 系统硬件主要由激光器(Surelite I-20, Continuum, 美国)、PCI4732数据采集卡(中科动态仪器公司)、步进旋转台及其电机控制箱(M600, 北京卓立汉光仪器有限公司)、前置放大器(5077PR, Olympus, 美国)、非聚焦超声探头(V310-SU, Olympus, 美国)和计算机等组成.

(ⅴ) 体外光声成像. 测量不同浓度下DA@Fe_2O_3纳米粒子的光声信号并与商用Au纳米颗粒光声造影剂作对比. DA@Fe_2O_3和Au纳米颗粒分别用去离子水稀释并调整浓度为8, 80, 800, 8000 μg/mL. 分别取制备好的样品各100 μL存放至内径0.9 mm, 外径1.2 mm的透明毛细管中, 然后将其嵌入制作好的仿体中. 扫描波长设置为532 nm, 脉冲宽度4~6 ns, 重复频率20 Hz, 步长为2°, 启动光声成像系统对其进行环形扫描. 每一组分别在相同参数下重复3次, 取其平均值作为输出信号以减小系统误差. 另外, 为进一步验证DA@Fe_2O_3纳米粒子和Au纳米颗粒的光声增强效果, 分别将相同浓度(80 μg/mL)的DA@Fe_2O_3和Au纳米颗粒的水溶液与等量的牛全血混合, 将制备好的样品放入上述透明毛细管中, 重复上述光声扫描过程.

(ⅵ) 小鼠大脑皮层光声成像. 选数只从山西医科大学动物中心购买的体重为25±5 g的健康雌性小鼠分为两组, 先进行短暂的气体麻醉, 随后腹腔内注射水合氯醛(10%), 剂量为0.04 mL/10 g. 待其彻底麻醉后, 剔除小鼠头部毛发, 实验组通过尾静脉注射100 μL浓度为80 μg/mL的DA@Fe_2O_3溶液, 空白组不

做任何处理. 然后将其固定在一个自制的光声系统容器中, 调整位置确保小鼠头部与超声探头的中心相平, 调整光斑大小与位置使其照射在小鼠两耳与两眼之间. 激光能量密度约11 mJ/cm^2, 低于人体皮肤最大允许辐射的激光能量密度20 mJ/cm^2[23]. 按照上述方法启动光声成像系统获得重建图像. 生物活体实验均经过太原理工大学动物实验管理小组委员会批准.

2 结果与讨论

2.1 类红细胞状Fe_2O_3纳米粒子的表征

图1为Fe_2O_3纳米颗粒的形貌、结构分析结果. 扫描电子显微镜(SEM)图像显示所制备Fe_2O_3纳米颗粒形貌均一, 呈规则的类红细胞状; 颗粒直径约为130±8 nm, 厚度为56±5 nm, 尺寸分布均匀(图1(a)). 图1(b)为所制备样品的X射线衍射(XRD)谱, 结果表明, 所有的衍射峰均可指认为斜方六面体氧化铁(α-Fe_2O_3, JCPDS No. 33-0664), 图谱中没有其他任何杂峰出现, 表明样品结晶相纯度较高. 图1(c)~(f)为样品的透射电子显微镜(TEM)表征结果, 从单个Fe_2O_3纳米颗粒的亮场像可以看出, 样品呈六角状. 选区电子衍射(SAED)结果(图1(d))表明, 样品为单晶、六角结构, 且具有较好的结晶度. 样品的高分辨图像(图1(e), (f))同样证明了上述结论, 并且结合电子衍射结果可以进一步给出晶体裸露晶面为{110}面(对应面间距为0.25 nm).

2.2 DA@Fe_2O_3对NIH3T3的毒性检测

通过MTT实验评价DA@Fe_2O_3的细胞毒性, 具体结果如图2所示. DA@Fe_2O_3对细胞活性的抑制率显示出对剂量和时间的依赖性, 各组间差异无统计学意义(P>0.05). NIH3T3细胞与DA@Fe_2O_3混合培养16 h后, 当DA@Fe_2O_3浓度由3.125 μg/mL增至200 μg/mL时, 相对细胞存活率从约96%降至约86%. 当NIH3T3细胞与DA@Fe_2O_3混合培养40 h后, DA@Fe_2O_3浓度从3.125 μg/mL增至200 μg/mL, 细胞相对存活率有8%的上下波动, 但均能保持在80%以上. 由此说明, DA@Fe_2O_3纳米粒子没有表现出明显的细胞毒性, 具有良好的生物相容性. 小鼠血常规检测(表S1), 及主要器官苏木精-伊红染色法(HE)染色组织学分析(图S1)结果也证明了上述结论.

2.3 DA@Fe_2O_3的体外光声成像

图3(a)是Fe_2O_3纳米粒子、DA@Fe_2O_3纳米粒子以及Au纳米颗粒的吸收光谱图. 其中, Fe_2O_3纳米粒子

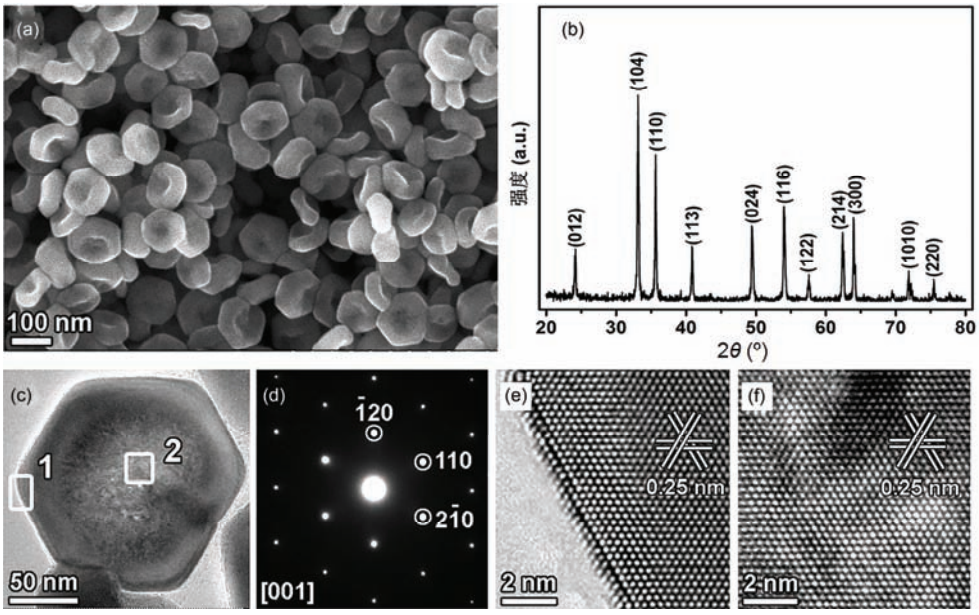

图 1 类红细胞状Fe_2O_3纳米粒子的形貌结构表征结果. (a) SEM; (b) XRD; (c) 亮场TEM图像; (d) SAED; (e), (f) 分别对应(c)中 1, 2 位置的高分辨TEM(HRTEM)图像

Figure 1 Typical morphology and structure of red blood cell-like-Fe_2O_3 nanoparticles. (a) SEM images. (b) XRD pattern. (c) Bright-field TEM image. (d) SAED pattern. (e), (f) HRTEM images of area 1 and 2 in (c)

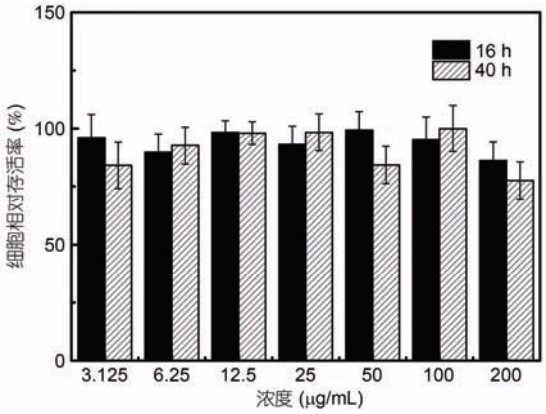

图 2 DA@Fe_2O_3对正常小鼠NIH3T3细胞的体外细胞毒性

Figure 2 *In vitro* cell cytotoxicity of DA@Fe_2O_3 to NIH3T3 cells

的吸收峰在560 nm, DA@Fe_2O_3纳米粒子的吸收峰为550 nm(相较未包覆多巴胺的Fe_2O_3纳米粒子蓝移10 nm), 商用Au纳米颗粒的吸收峰在525 nm, 三种材料的吸收峰均位于激发光共振范围内. 不同浓度Fe_2O_3纳米颗粒、DA@Fe_2O_3纳米颗粒与商用Au纳米颗粒水溶液的光声信号对比如图3(b)所示. 随纳米颗粒浓度的增加(0~8000 μg/mL), 三种造影剂材料的光声信号均呈e指数增强. 但是, 相比同浓度的Fe_2O_3纳米颗粒和Au纳米颗粒, 本文所制备DA@Fe_2O_3光声造影剂产生的光声信号幅值分别提高约25%和30%. 图3(c)是浓度为80 μg/mL的Fe_2O_3纳米粒子、DA@Fe_2O_3纳米粒子和商用Au纳米颗粒的牛全血溶液的光声信号测量结果. 可以看出, 牛全血中加入Fe_2O_3纳米颗粒、DA@Fe_2O_3纳米颗粒和商用Au纳米颗粒后光声信号幅值分别增强了约74%, 84%和70%, 相较于未修饰的Fe_2O_3纳米颗粒和商用的Au纳米颗粒, DA@Fe_2O_3纳米粒子的光声造影增强效果分别提高了13%和20%. 实验结果反映出DA@Fe_2O_3纳米粒子作为光声成像造影剂进行体内实验的潜质(表S2, 图S2).

2.4 DA@Fe_2O_3用于小鼠大脑皮层光声成像

图4为DA@Fe_2O_3纳米粒子、Fe_2O_3纳米粒子和Au纳米粒子应用于小鼠大脑皮层血管光声成像的实验分析结果. 注射DA@Fe_2O_3(图4(b), (c)), Fe_2O_3(图4(f), (g))和Au(图4(j), (k))光声造影剂前后小鼠大脑皮层血管的光声重建图像如图4所示, 从图中可以看出, 3种造影剂注射前, 虽然血管成像轮廓清晰, 但图像对比度偏低; 而注射造影剂之后, 小鼠大脑皮层血管清晰可见, 且成像对比度明显得到增强. 调取小鼠大脑皮

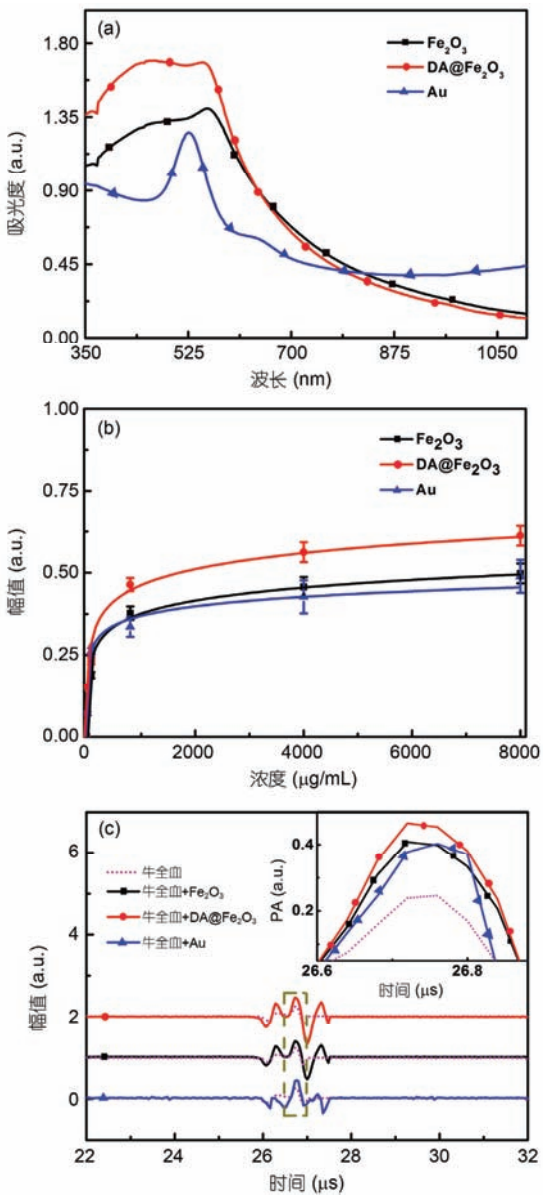

图 3 (网络版彩色)Fe_2O_3, DA@Fe_2O_3和Au的体外光声特性测量结果. (a) Fe_2O_3, DA@Fe_2O_3和Au纳米球的可见光-红外(Vis-IR)吸收谱; (b) 不同浓度(0~8000 μg/mL)的Fe_2O_3, DA@Fe_2O_3和Au纳米球水溶液的光声信号测量结果; (c) 浓度80 μg/mL的Fe_2O_3, DA@Fe_2O_3和Au纳米球的牛全血溶液的光声信号测量结果

Figure 3 (Color online) The photoacoustic properties of Fe_2O_3, DA@Fe_2O_3 and Au *in vitro*. (a) Vis-IR spectrum of Fe_2O_3, DA@Fe_2O_3 and Au nanospheres in water. (b) PA signals from Fe_2O_3, DA@Fe_2O_3 and Au nanospheres at various concentrations (0–8000 μg/mL). (c) PA signals generated from Fe_2O_3, DA@Fe_2O_3 and Au nanospheres suspension at concentration of 80 μg/mL mixed with blood

层中动脉血管的原始光声信号图4((d),(h),(l))进行比对计算, 结果发现, 注射DA@Fe_2O_3, Fe_2O_3和Au造影剂后光声信号幅值相比注射造影剂前分别增强了约

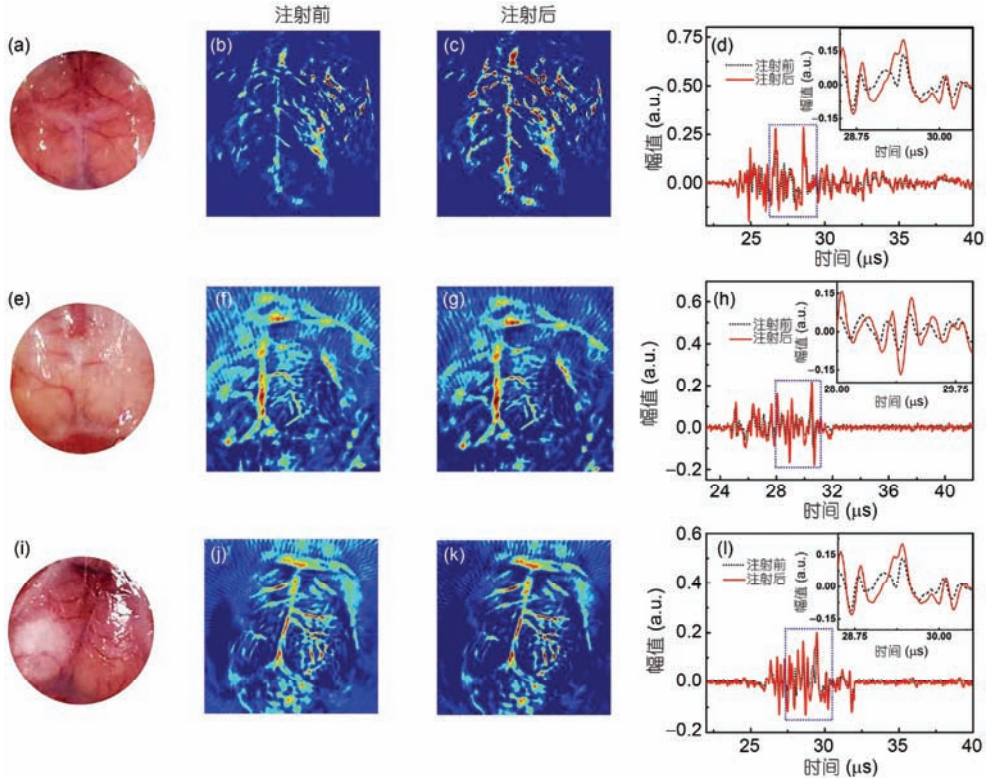

图 4 (网络版彩色)DA@Fe_2O_3, Fe_2O_3 和Au用于小鼠大脑皮层光声成像的测量结果. (a), (e), (i) 小鼠的大脑皮层解剖实物图. 注射前((b), (f), (j)) 和注射后((c), (g), (k))的小鼠大脑皮层血管光声成像图. (d), (h), (l) 小鼠大脑皮层的中动脉血管的光声信号强度对比. (a)~(d) DA@Fe_2O_3; (e)~(h) Fe_2O_3; (i)~(l) Au

Figure 4 (Color online) Comparison of measurement results of DA@Fe_2O_3, Fe_2O_3 and Au in photoacoustic imaging of mouse cortical. (a), (e), (i) Dissected photograph of the small rat brain applied in the PAT experiment. PAT images produced by the middle cerebral artery of a rat brain before ((b), (f), (j)) and after ((c), (g), (k)) DA@Fe_2O_3, Fe_2O_3 and Au injection. (d), (h), (l) Comparison chart of PA signals. (a)–(d) DA@Fe_2O_3; (e)–(h) Fe_2O_3; (i)–(l) Au

65%, 58%和50%. 图4(a), (e), (i)为小鼠的大脑皮层解剖实物图, 光声重建图像与其在结构上基本吻合. 实验结果表明, 具有强吸收特性的Fe_2O_3纳米材料可以作为光声造影剂以提高光声成像技术的灵敏度.

3 结论

本文成功制备了盐酸多巴胺修饰的类红细胞状Fe_2O_3纳米光声造影剂, 并对DA@Fe_2O_3造影剂的光声成像特性进行了全面系统的评估. 首先, DA@Fe_2O_3对正常小鼠胚胎成纤维细胞没有明显毒性; 其次, 体外实验表明, 在532 nm激光的激发下, DA@Fe_2O_3纳米粒子相较商用金纳米颗粒具有更强的光声效应; 最后, 小鼠大脑皮层血管成像实验证实通过添加DA@Fe_2O_3光声造影剂, 光声信号相较不添加造影剂强度提高了65%, 光声重建图像的信噪比和对比度得以明显提升. 综上所述, DA@Fe_2O_3纳米粒子生物兼容性良好, 且体内体外实验都表现出较强的光声造影效果, 具有作为高性能光声造影剂的潜质.

参考文献

1 Kircher M F, Willmann J K. Molecular body imaging: MR imaging, CT, and US. Part I. Principles. Radiology, 2012, 263: 633–643
2 Emelianov S Y, Li P C, O'Donnell M. Photoacoustics for molecular imaging and therapy. Phys Today, 2009, 62: 34–39
3 Petrov I Y, Petrov Y, Prough D S, et al. Optoacoustic monitoring of cerebral venous blood oxygenation though intact scalp in large animals. Opt Express, 2012, 20: 4159–4167
4 Yang S H, Xing D, Xiang L Z. Photoacoustic and thermoacoustic tomography and functional imaging for brain structure (in Chinese). Sci China Ser G: Phys Mechan Astron, 2007, 37: 101–109 [杨思华, 邢达, 向良忠. 基于光声、热声技术的脑组织结构及功能成像.

中国科学 G 辑: 物理学 力学 天文学, 2007, 37: 101–109]
5 Xi L, Grobmyer S R, Zhou G, et al. Molecular photoacoustic tomography of breast cancer using receptor targeted magnetic iron oxide nanoparticles as contrast agents. J Biophoton, 2014, 7: 401–409
6 Cook J R, Frey W, Emelianov S. Quantitative photoacoustic imaging of nanoparticles in cells and tissues. ACS Nano, 2013, 7: 1272–1280
7 Zhang T, Cui H, Fang C Y, et al. Photoacoustic contrast imaging of biological tissues with nanodiamonds fabricated for high near-infrared absorbance. J Biomed Opt, 2013, 18: 026018
8 Shin T H, Choi Y, Kim S, et al. Recent advances in magnetic nanoparticle-based multi-modal imaging. Chem Soc Rev, 2015, 44: 4501–4516
9 Wu X, Wang Z G, Xu C S. Progress of study on nano-scale contrast agents for ultrasonic molecular imaging and targeted therapy (in Chinese). Chin J Ultrasonogr, 2006, 7: 539–540 [伍星, 王志刚, 许川山. 纳米级造影剂在超声分子显像与靶向治疗中的研究进展. 中华超声影像学杂志, 2006, 7: 539–540]
10 Kim C, Cho E C, Chen J, et al. *In vivo* molecular photoacoustic tomography of melanomas targeted by bioconjugated gold nanocages. ACS Nano, 2010, 4: 4559–4564
11 Kang B, Yu D, Dai Y, et al. Cancer-cell targeting and photoacoustic therapy using carbon nanotubes as “Bomb” agents. Small, 2009, 5: 1292–1301
12 Yang K, Zhang S, Zhang G, et al. Graphene in mice: Ultrahigh *in vivo* tumor uptake and efficient photothermal therapy. Nano Lett, 2010, 10: 3318–3323
13 Liu T, Shi S, Liang C, et al. Iron oxide decorated MoS_2 nanosheets with double PEGylation for chelator-free radio labeling and multi-modal imaging guided photothermal therapy. ACS Nano, 2015, 9: 950–960
14 Cheng L, Liu J, Gu X, et al. PEGylated WS_2 nanosheets as a multifunctional theranostic agent for *in vivo* dual-modal CT/Photoacoustic imaging guided photothermal therapy. Adv Mater, 2014, 26: 1886–1893
15 Dai F, Du M, Liu Y, et al. Folic acid-conjugated glucose and dextran coated iron oxide nanoparticles as MRI contrast agents for diagnosis and treatment response of rheumatoid arthritis. J Mater Chem B, 2014, 2: 2240–2247
16 Lee N, Choi Y, Lee Y, et al. Water-dispersible ferrimagnetic iron oxide nanocubes with extremely high r_2 relaxivity for highly sensitive *in vivo* MRI of tumors. Nano Lett, 2012, 12: 3127–3131
17 Song X, Gong H, Yin S, et al. Ultra-small iron oxide doped polypyrrole nanoparticles for *in vivo* multimodal imaging guided photothermal therapy. Adv Funct Mater, 2014, 24: 1194–1201
18 Zhou T, Wu B, Xing D. Bio-modified Fe_3O_4 core/Au shell nanoparticles for targeting and multimodal imaging of cancer cells. J Mater Chem, 2012, 22: 470–477
19 Xie J, Chen K, Huang J, et al. PET/NIRF/MRI triple functional iron oxide nanoparticles. Biomaterials, 2010, 31: 3016–3022
20 Mazur M, Barras A, Kuncser V, et al. Iron oxide magnetic nanoparticles with versatile surface functions based on dopamine anchors. Nanoscale, 2013, 5: 2692–2702
21 Martín M, Salazar P, Jiménez C, et al. Rapid Legionella pneumophila determination based on a disposable core-shell Fe_3O_4@poly(dopamine) magnetic nanoparticles immunoplatform. Anal Chim Acta, 2015, 887: 51–58
22 Baig R B N, Leazer J, Varma R S. Magnetically separable Fe_3O_4@DOPA-Pd: A heterogeneous catalyst for aqueous Heck reaction. Clean Technol Environ Policy, 2015, 17: 2073–2077
23 Laser Institute of America. American National Standard for Safe Use of Lasers. ANSI Z1361, 2000

补充材料

表 S1 小白鼠血常规检测各参数指标
表 S2 Fe_2O_3 和 DA@Fe_2O_3 纳米粒子在水溶液和血清中的粒径和表面电荷
图 S1 实验组和空白组小鼠主要器官切片的 H&E 染色
图 S2 Fe_2O_3 和 DA@Fe_2O_3 的 TEM 图

本文以上补充材料见网络版 csb.scichina.com. 补充材料为作者提供的原始数据, 作者对其学术质量和内容负责.

Summary for “类血红细胞状氧化铁纳米颗粒在小鼠大脑皮层光声成像中的应用”

Red blood cell-like-Fe_2O_3 nanocrystals as contrast agents for PAT on a rat cerebral cortex *in vivo*

HE ZaiQian[1], WANG YiPing[1], YAN XiaoLe[1], YANG MinMin[1], WANG Ying[2], LI PengWei[1*], JIANG HuaBei[3] & ZHANG WenDong[1]

[1] *Ministry of Education Key Laboratory of Advanced Transducers and Intelligent Control System, Micro-Nano System Research Center of College of Information Engineering, Taiyuan University of Technology, Taiyuan 030024, China;*
[2] *Biological Engineering of Mechanics Institute, Taiyuan University of Technology, Taiyuan 030024, China;*
[3] *Department of Medical Engineering, University of South Florida, Tampa, 32611, USA*
* Corresponding author, E-mail: lipengwei@tyut.edu.cn

Photoacoustic tomography (PAT) is a novel, noninvasive, nonionizing and cost-effective imaging modality, which combines the merits of optical and ultrasonic imaging, and has been recently prosperous for biomedical applications. Owing to the high optical absorption of hemoglobin this endogenous molecules contrast agent, PAT has been confirmed to be a mighty imaging tool for blood vessels. With the development of science and technology, nanotechnology has increasingly been brought to the forefront due to the unique physical and chemical properties of nanomaterials, such as small size effect, surface and interface effects. During the past few decades, nanoparticles designed for high photoacoustic contrast agents have become a burgeoning scientific favorite. Iron oxide has been extensively investigated because of good magnetic properties, thermal and chemical stability as well as its low cost, easy and environmentally friendly. Especially, due to its good compatibility and hypotoxicity, it has been widely used in nuclear magnetic resonance imaging (MRI) contrast agents. Besides, many functional groups (cathecol, amine, quinone) of dopamine hydrochloride (DA) can be reacted with a large number of molecules so as to provide a friendly method to make many bio-molecules tightly immobilized on the surface.

Red blood cell-like-Fe_2O_3 nanoparticles modified by DA (DA@Fe_2O_3) were prepared in order to be utilized as an optical contrast agent in PAT. Red blood cell-like-Fe_2O_3 nanoparticles were synthesized by a facile hydrothermal synthesis method and modified by dopamine hydrochloride. The cell toxicity of DA@Fe_2O_3 was surveyed by incubating with NIH3T3 cells using MTT assy. The *ex vivo* photoacoustic performance of DA@Fe_2O_3 was tested by using a transparent tube containing only suspensions with a range of concentrations and mixed with blood by PAT system. DA@Fe_2O_3 as contrast agent in photoacoustic tomography of a rat cerebral cortex was also observed. DA@Fe_2O_3 has not shown any significant cell growth inhibition at concentrations ranging from 3.125 to 200 μg/mL. PA contrast enhancement properties *in vitro* of DA@Fe_2O_3 got more remarkable with the concentration of nanoparticles increasing. The contrast of PAT images of the cerebral cortex of a rat after DA@Fe_2O_3 aqueous suspension at a specific concentration injection through the tail was enhanced.

DA@Fe_2O_3 shows hypotoxicity and good biological compatibility. DA@Fe_2O_3 presents a strong absorption to the specific wavelength laser and excellent PA contrast enhancement properties *in vitro* and *in vivo*. These results demonstrated that DA@Fe_2O_3 could be utilized as innovative, commercially viable, promising candidates as alternative optical contrast agents.

Fe_2O_3 nanocrystals, contrast agent, photoacoustic tomography

doi: 10.1360/N972016-01455